

1 **Measurement Report: Urban Ammonia and Amines in Houston, Texas**

2
3 Lee Tiszenkel¹, James Flynn², Shan-Hu Lee^{1*}

4
5 ¹ Department of Atmospheric and Earth Sciences, University of Alabama at Huntsville;
6 Huntsville, Alabama, USA

7 ² Department of Earth and Atmospheric Sciences, University of Houston; Houston, Texas,
8 USA

9
10 Corresponding author (shanhu.lee@uah.edu)

11

12 **Abstract.** Ammonia and amines play critical roles in secondary aerosol formation, especially in
13 urban environments. However, fast measurements of ammonia and amines in the atmosphere are
14 very scarce. We measured ammonia and amines with a chemical ionization mass spectrometer
15 (CIMS) at the urban center in Houston, Texas, the fourth most populated urban site in the United
16 States, during October 2022. Ammonia concentrations were on average 4 parts per billion in
17 volume (ppbv), while the concentration of an individual amine ranged from several parts per
18 trillion in volume (pptv) to hundreds of pptv. These reduced nitrogen compounds were more
19 abundant during the weekdays than on weekends and correlated with measured CO concentrations,
20 implying they were mostly emitted from pollutant sources. Both ammonia and amines showed a
21 distinct diurnal cycle, with higher concentrations in the warmer afternoon, indicating dominant
22 gas-to-particle conversion processes taking place with the changing ambient temperatures. Studies
23 have shown that dimethylamine is critical for new particle formation (NPF) in the polluted
24 boundary layer, but currently, there are no amine emission inventories in global climate models
25 (as opposed to ammonia). Our observations made in very polluted Houston, as well as a less
26 polluted site (Kent, Ohio) from our previous study (You et al., 2014), indicate there is a consistent
27 ratio of dimethylamine over ammonia at these two sites. Thus, our observations can provide a
28 relatively constrained proxy of dimethylamine using 0.1% ammonia concentrations at polluted
29 sites in the United States to model NPF processes.

Deleted: urban

Deleted: [You et al., 2014]Our observations show that amines in general positively correlated with ammonia, indicating that it is reasonable for global models to use scaled-down ammonia concentrations (e.g., 0.1 %) as a proxy of urban dimethylamine concentrations to simulate urban NPF processes.

30 1. Introduction

31 Atmospheric ammonia and amines are ubiquitous in the atmosphere, and they have been found
32 in the gas phase, aerosol, clouds, and fog droplets (Ge et al., 2011a, b). Ammonia and amines are
33 emitted from various natural and anthropogenic sources, such as agricultural activity, animal
34 husbandry, vegetation, soil, waste processing, automobile traffic, power plants, and biomass
35 burning (Ge et al., 2011a). Ammonia and amines often share the same emission sources. In general,
36 ambient concentrations of ammonia are at the parts per billion in volume (ppbv) range, and amines
37 are approximately two to three orders of magnitude lower than ammonia concentrations. Ambient
38 concentrations of ammonia and amines vary rapidly due to emission, gas-to-particle conversion,
39 and wet deposition processes (You et al., 2014; Yu and Lee, 2012).

Deleted: [Ge et al., 2011a; b]

40 Laboratory studies have shown that ammonia and amines play key roles in new particle
41 formation (NPF) as they can stabilize sulfuric acid clusters (Yu et al., 2012; Almeida et al., 2013;
42 Lehtipalo et al., 2018; Xiao et al., 2021; Glasoe et al., 2015; Jen et al., 2016). In particular,
43 dimethylamine can have a profound effect on atmospheric processes even at the pptv level
44 (Almeida et al., 2013; Glasoe et al., 2015). Field observations show that ammonia and amines are
45 associated with NPF events in Chinese megacities (Yao et al., 2016; Yan et al., 2021; Cai et al.,
46 2021; Cai et al., 2023), urban areas in the United States (Jen et al., 2016; Smith et al., 2010),
47 European cities (Brean et al., 2020), a high altitude site (Bianchi et al., 2016), and the Arctic and
48 Antarctic (Beck et al., 2021; Brean et al., 2021; Jokinen et al.; Köllner et al., 2017). However,
49 global models cannot simulate urban NPF processes currently because of the lack of amine
50 emission inventories in models.

58 Ammonia and amines also contribute to secondary organic aerosol (SOA) formation by
59 condensation of oxidation products formed by reactions with ozone, OH, or NO₃ radicals and
60 produce light-absorbing particles (Erupe et al., 2010; Malloy et al., 2009; Silva et al., 2008;
61 Nielsen, 2016; Nielsen et al., 2012; Qiu and Zhang, 2013). As a result, reducing ammonia
62 emissions has been identified as a cost-effective way to mitigate ambient fine particle
63 concentrations (Gu et al., 2021).

64 Fast-response measurements of ammonia and amines at atmospheric concentrations are very
65 challenging (Lee, 2022), although such measurements are necessary because these reduced
66 nitrogen compounds have relatively short atmospheric lifetimes (Nielsen et al., 2012). Previously,
67 (Schwab et al., 2007) made an intercomparison of six different ammonia detection methods in the
68 laboratory and found a large variance in the measured concentrations and vastly different response
69 times (over several hours) within different instruments. Difficulties in the detection of base
70 compounds also arise because these “sticky” compounds can rapidly adsorb and desorb on/from
71 the surfaces of sampling inlets to cause background signals that vary depending on ambient
72 concentrations, air humidity, and other atmospheric conditions. Thus frequent, in situ
73 measurements of instrument background signals using proper zero gases are required, especially
74 for field observations with rapidly changing ambient concentrations of base compounds.

75 Chemical ionization mass spectrometers (CIMS) using ion reagents such as protonated ethanol,
76 acetone, and water ions can detect ammonia and amines in the atmosphere with fast response
77 (Nowak et al., 2006; Benson et al., 2010; Yu and Lee, 2012 ; Hanson et al., 2011; Jen et al., 2016;
78 Nowak et al., 2010). As summarized in Table 1, CIMS technique has been used for the detection
79 of ambient ammonia and amines at a polluted site in Ohio (You et al., 2014; Yu and Lee, 2012),
80 a rural Alabama forest (You et al., 2014), and polluted urban sites in China (Zheng et al., 2015;
81 Wang et al., 2020a; Wang et al., 2016; Zhu et al., 2022). As shown in Table 1, there are even fewer
82 studies that simultaneously measured ammonia and amines. The CIMS using ethanol reagent can
83 measure amines at or below single-digit pptv concentrations with a time response of 1 minute and
84 measure simultaneously amines and ammonia (You et al., 2014; Yu and Lee, 2012 ; Erupe et al.,
85 2011; Benson et al., 2010). The CIMS using protonated water ions (i.e., proton-transfer chemical
86 ionization mass spectrometer, PTR-CIMS) can measure mono- and di-amines (Hanson et al., 2011;
87 Jen et al., 2016). Using a high-resolution time-of-flight (HR-TOF) detector coupled to CIMS (HR-
88 TOF CIMS) (with ethanol reagent), (Yao et al., 2016) measured various amines and amides in
89 Shanghai. However, isomers of amines were still not resolved in the detection; for example, the
90 measured C₂-amines still contained dimethylamine and ethylamine. Thus, a major disadvantage
91 of a mass spectrometer (regardless of mass resolution) is the inability to resolve/identify isomers.
92 To resolve isomers, tandem MS/MS analysis or an additional independent separation method (such
93 as chromatography) coupled to the mass spectrometer is necessary.

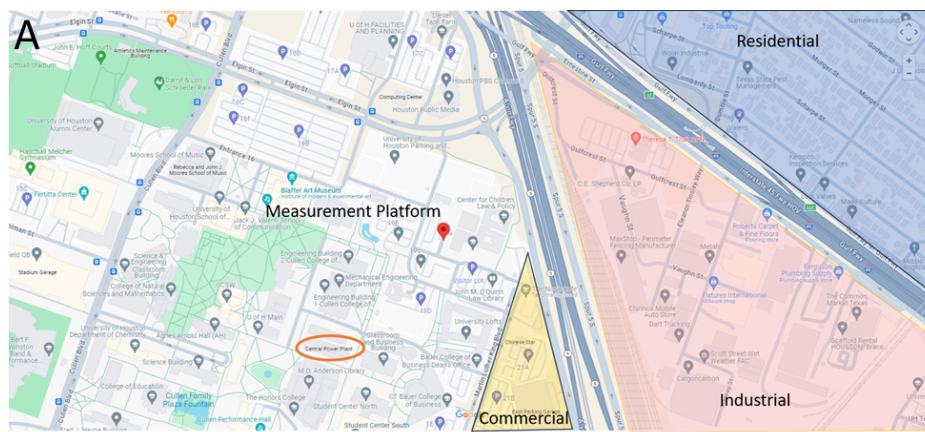
94 In situ measurements of ammonia have been made in various atmospheric environments also
95 with optical techniques such as open-path absorption (Miller et al., 2014), closed-path absorption
96 (Griffith and Galle, 2000; Ellis et al., 2010; Mcmanus et al., 2010; Leen et al., 2013; Pollack et al.,
97 2019), cavity ring-down spectroscopy (Martin et al., 2016), and photoacoustic spectroscopy

98 (Pushkarsky et al., 2002). These fast-response optical techniques were used for flux and aircraft
99 measurements of ammonia.

100 We measured ammonia and C1-C6 amines with an ethanol CIMS in October 2022 at the urban
101 center in Houston, Texas. Houston is the fourth most populated urban center in the U.S. and
102 contains a diverse range of pollutant emissions from urban activity, traffic, ship channels, oil
103 production, marine air masses, and agricultural activity. The primary goal of these measurements
104 is to quantify ammonia and C1-C6 amines in an urban setting and identify the atmospheric
105 conditions that affect their abundance. The study is amongst very few observations of ammonia
106 and amines at highly polluted urban sites in the U.S. We also compare observations in Houston
107 with previous measurements taken with the same instrument in Kent, Ohio (less polluted) (You et
108 al., 2014) and establish a quantitative relationship between ammonia and dimethylamine in a
109 different range of polluted conditions. This relationship will allow global models to simulate urban
110 NPF processes using the existing ammonia emission inventories.

111
112
113

2. Methods



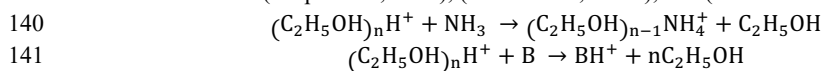
114
115
116
117
118
119
120
121

Figure 1. Location of the measurement platform, indicated by a red pin in the center of the map. Nearby commercial, industrial, and residential areas are labeled by yellow, red, and blue shaded sections, respectively. The nearby University of Houston power plant is circled in orange to the southwest of the measurement platform. The map of the greater Houston urban area, as well as the satellite view of the nearby vicinity of the measurement site, are shown in Figure S1.

122 The field observation took place in Houston continuously from the 8th to the 27th of October in
123 2022. Measurements were made at a stationary platform located on the campus of the University
124 of Houston (29.72° N, 95.34° W) ~2.5 km from central downtown Houston. Maps of the
125 measurement site (Figures 1 and S1). The measurement platform was located ~5 m from an active

126 parking lot, ~200 m from a low-traffic road, ~300 m from a high-traffic thoroughfare, and ~500 m
127 from an interstate highway. The immediate vicinity of the site was the University of Houston
128 campus, containing classroom buildings, dormitories, facilities services, and dining halls. Nearby
129 to the southeast of the site were several restaurants as well as an industrial park containing sites of
130 chemical supply companies, construction, machining services, and automobile shops. The site was
131 surrounded by residential areas to the south, northeast, and west. The city center and highest
132 population densities were to the northeast of the measurement site.

133
134 The ethanol CIMS instrument used has been described in detail previously (Benson et al.,
135 2010; You et al., 2014; Yu and Lee, 2012). The CIMS draws 10 standard liter per minute (slpm)
136 of sample air into a low-pressure ion-molecule region (about 2,000 Pa) where the flow mixes with
137 a pure nitrogen flow with a 2 slpm through a stainless-steel vessel of 200-proof ethanol, followed
138 by a ^{210}Po radiation source. Ammonia and amines were detected with the following ion-molecule
139 reactions based on (Erupe et al., 2011), (Yu and Lee, 2012), and (Nowak et al., 2006):



142 Here, “B” refers to amines, and “n” is the number of reagent ions measured by the CIMS (n=1-3).
143 The $(\text{C}_2\text{H}_5\text{OH})_2\text{H}^+$ (m/z = 93) peak was the highest among the three reagent ions (m/z = 47, 93,
144 and 140). As shown in Figure S2, the production ions of amines were protonated ions: C1-amine
145 (m/z = 32), C2 (m/z = 46), C3 (m/z = 60), C4 (m/z = 74), C5 (m/z = 88), and C6 (m/z = 102).
146 Ammonia product ions were NH_4^+ (m/z = 18, higher peak) and $(\text{C}_2\text{H}_5\text{OH})\text{NH}_4^+$ (m/z = 64, lower
147 peak); these two ions were strongly correlated to each other during the ammonia calibration and
148 ambient measurements, indicating they represent ammonia signals.

149 To obtain a background signal, the CIMS is operated with 10 minutes of sampling followed
150 by 10 minutes of background measurements. Figure S2 shows the main reagent and base
151 compound product ions during the switching between ambient and background measurements.
152 Background measurements were taken by switching a 3-way valve to supply the inlet with a flow
153 of zero air through a silicon phosphate medium (Pan Tech, Texas) to scrub ammonia and amines.
154 The reagent signal was taken as the sum of three ethanol reagent ions. Reagent ion signals were
155 typically around 400 kHz with less than 10 % difference between ambient and background
156 measurement modes. Ammonia and amine concentrations were calculated by the difference
157 between the ambient and background signals normalized to 1,000,000 Hz of reagent ion signal
158 multiplied by a calibration factor. Calibration of the instrument was carried out with diluted
159 ammonia in nitrogen and permeation tubes of methylamine, dimethylamine, trimethylamine,
160 diethylamine, and diisopropylamine (Kin-tek, USA). Due to the difficulty of obtaining a
161 calibration standard, C5 amines were assumed to have the same sensitivity as C6 amines. The
162 calibration factors for each compound and detection limits were found to be similar to the results
163 from the calibration of the instrument by (You et al., 2014) (Table S1), over a period of nearly 10
164 years, demonstrating an excellent reproducibility in the instrument performance. The time
165 response of the CIMS instrument to ammonia and amines is defined as where the signal stabilizes

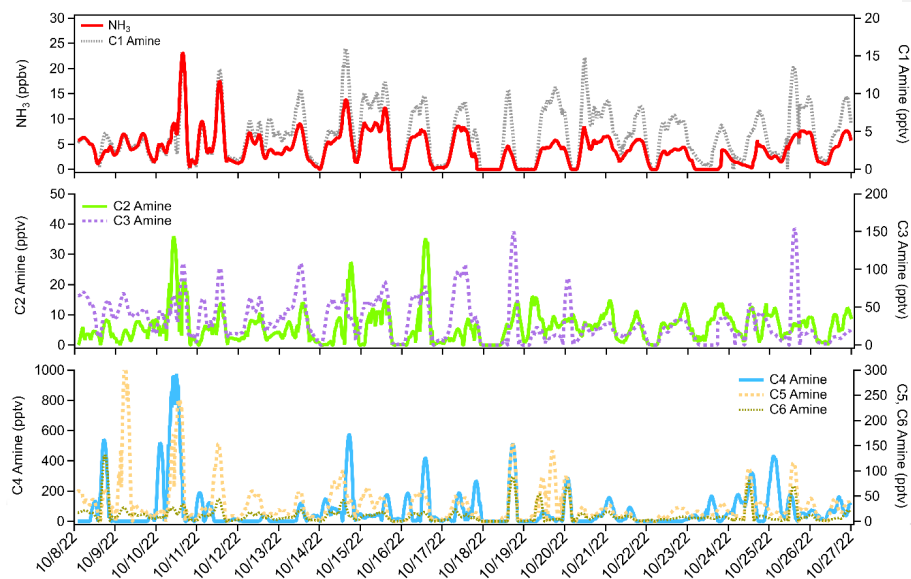
166 at its “double e-folded” concentration of $1/e^2$ during the calibration. Average response times for
167 ammonia and amines were smaller than 1 minute. For each 10-minute cycle of background and
168 measurement, the first two minutes of each background/measurement cycle were excluded from
169 the data analysis to allow the instrument to reach a steady concentration.

170 The uncertainty in the CIMS included error in the permeation sources, which ranged from 2%
171 to 5% depending on the compound. The permeation sources were diluted in two stages using flow
172 controllers that each had uncertainties of 1.5%. Total error in the calibration of the CIMS was
173 6.7%. Overall uncertainty in the CIMS was 30%, accounting for calibration error, variability of
174 ion signals, and inlet losses.

175 Meteorological data was measured concurrently on the platform by a Vaisala HMP-45c for
176 temperature and relative humidity, and a RM Young 05305 wind speed and direction sensor.
177 Additionally, CO and NO_x (NO+NO₂) were measured with Thermo 48c and Thermo 42c-TL,
178 respectively. These measurements were provided by the University of Houston. The uncertainty
179 in trace gas (CO and NO_x) measurements arises from instrumental uncertainty in the Thermo 48c
180 CO analyzer and Thermo 42c-TL NO_x analyzer. Zero correction was performed on this instrument
181 daily by switching to a flow of zero air. The typical uncertainty of each of these instruments was
182 5%.

183
184
185
186

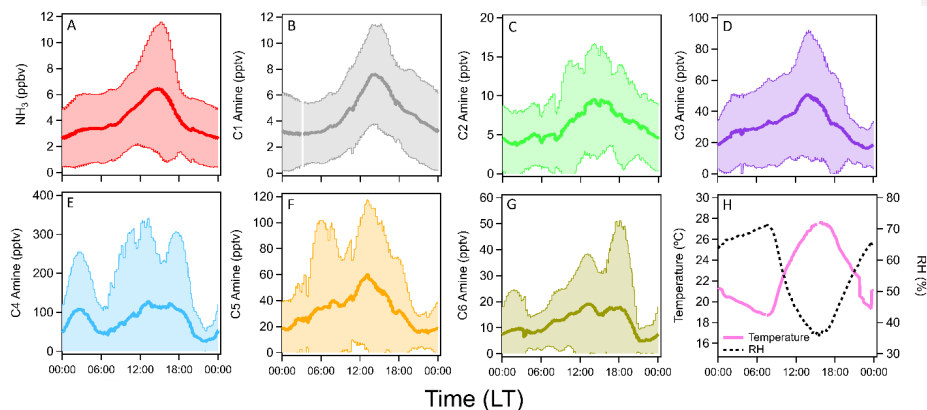
3. Results and Discussion



187

188 **Figure 2.** Time series of ammonia and C1-C6 amines observed at the urban center in Houston,
189 Texas, in October 2022.

190 The time series of ammonia and amines during the ambient measurement period is shown in
191 Figure 2. The average ammonia concentration during the measurement campaign was 4 ppbv with
192 several short-term spikes above 10 ppbv and one occasion when the concentration exceeded 20
193 ppbv. Concentrations of C1 amine averaged 4 pptv with several spikes up to 15 pptv. Average C2
194 amine concentrations were 6 pptv with frequent but brief periods of concentrations more than 10
195 pptv. Average C3 amine concentrations were 31 pptv with brief increases in concentration above
196 100 pptv. C4 amine was the most abundant amine observed during the measurement period with
197 an average concentration of 79 pptv with spikes in concentration into the hundreds of pptv.
198 Average C5 and C6 amine concentrations were 33 and 12 pptv, respectively. These concentrations
199 in Houston were generally consistent with concentrations measured in other urban sites (Table 1).
200 Previous CIMS ammonia measurements from aircraft flights above Houston observed similar
201 baseline concentrations of ammonia (0.2-3 ppbv) with brief spikes in concentration (up to 80 ppbv)
202 associated with agricultural or industrial activity (Nowak et al., 2010). Additionally, ammonia
203 concentrations of similar magnitude to the high spikes in concentration observed in this study have
204 been reported in Shanghai (Xiao et al., 2015) as well as an urban site in Romania (Petrus et al.,
205 2022), with high ammonia concentrations corresponding to high temperatures and high traffic
206 activity. Long-term measurements taken in Nanjing with a cavity ring-down spectrometer also
207 showed an average ammonia concentration of 12 ppbv (Liu et al., 2024). Measurements of amines
208 in Atlanta, Georgia showed <1 to 3 pptv concentrations of C1 and C2 amines, and C3 and C6
209 amines up to 15-25 pptv (Hanson et al., 2011). Yao et al. (Yao et al., 2016) measured amines at
210 the level of pptv or sub-pptv, e.g., C2 amines of 3.9 ± 1.2 pptv, in urban Shanghai during the
211 summer. It is possible that measured concentrations of amines measured here contain some
212 interference from amides formed from oxidation of emitted amines. The CIMS does not have
213 sufficient resolving power to separate trimethylamine (m/z 59.11) from acetamide (m/z 59.07), for
214 example. Therefore, these amine concentrations represent an upper limit of amine concentrations
215 (assuming all of the detected signal is due to the presence of amines). However, (Yao et al., 2016)
216 measured amide concentrations in urban Shanghai in the tens to hundreds of pptv, while C1-C2
217 amine concentrations in Shanghai were similar to Houston observations reported here. Considering
218 the consistency between amine measurements at these two urban locations, it is likely that
219 interference from amides in the CIMS was minimal for C1 and C2 amines. The discrepancies
220 between these two urban areas become more pronounced for C3-C6 amines (Table 1), which
221 makes amide interference a possible explanation for elevated concentrations of C3 amines and
222 above.
223



224

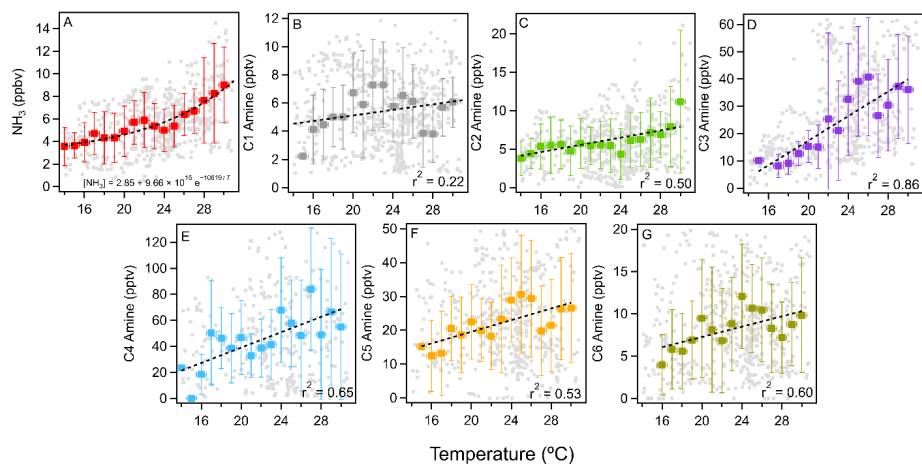
225 **Figure 3.** Averaged diurnal cycles of (a) ammonia, (b-g) C1-C6 amines, (h) temperature, and RH
 226 in Houston, Texas, during the observation period (19 days continuously). Shaded areas indicate 1
 227 standard deviation from the mean values of observation data.

228 Figure 3 shows the averaged diurnal concentrations of ammonia and amines during the
 229 observation period. Ammonia and amines had a diurnal cycle with peak concentrations in the
 230 afternoon with higher ambient temperatures. Generally, ammonia and amines correlated with one
 231 another throughout the measurement campaign, while C1-C3 amines showed the highest
 232 correlation with ammonia. Peak concentrations of all compounds corresponded with the high
 233 temperature of the day at around 3 pm local time. This was especially pronounced for ammonia,
 234 C1 and C3 amines. The relationships between ammonia and amines and temperature are shown in
 235 Figure 4. Ammonia had the strongest correlation with temperature, and the relationship fit an
 236 exponential parameterization, as the following:

$$237 \quad [NH_3] = 2.85 + 9.66 \times 10^{15} e^{-\frac{10619}{T}}$$

238 Amines generally showed linear relationships with temperature, with C3 and C4 amines displaying
 239 the strongest relationships. C3 amines increased by 2.3 pptv per °C ($r^2 = 0.86$) and C4 by 2.9 pptv
 240 per °C ($r^2 = 0.65$). C5 and C6 amines were also moderately correlated with temperature, increasing
 241 by 1.2 pptv per °C and 0.5 pptv per °C, respectively ($r^2 = 0.60$ for both C5 and C6). On the other
 242 hand, the correlation of C1 and C2 amines with temperature were weaker: C1 only increased by
 243 0.1 pptv per °C with almost no correlation ($r^2 = 0.22$), and C2 increased by 0.8 pptv per °C ($r^2 =$
 244 0.50). The temperature dependence of ammonia and amines was previously observed in a rural
 245 forest in Alabama by (You et al., 2014), which attributed this partially to particle-to-gas conversion
 246 of ammonia and amine containing particles at elevated temperatures. The temperature dependence
 247 could also be due to higher emissions at higher temperatures. The temperature dependence of
 248 ammonia and amines has been observed at other urban, suburban and rural locations such as Kent,

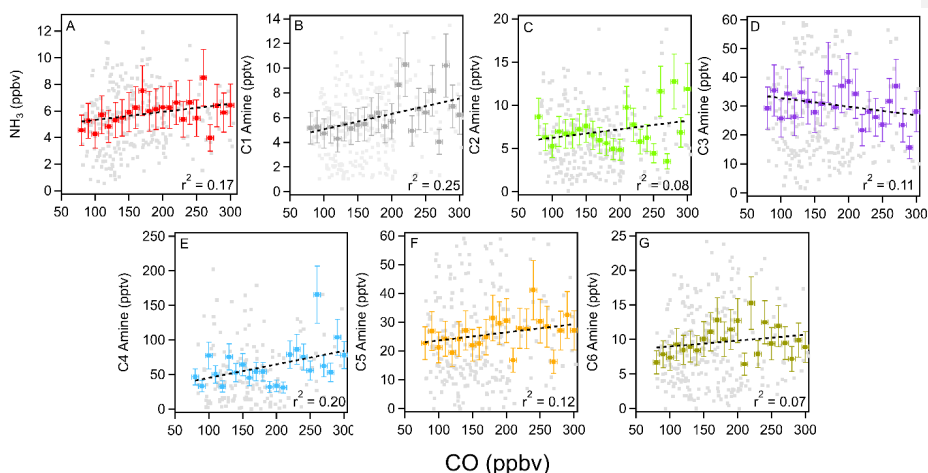
249 Ohio (You et al., 2014), Atlanta (Hanson et al., 2011), Delaware (Freshour et al., 2014), the
 250 Southern Great Plains (Freshour et al., 2014), and rural central Germany (Kürten et al., 2016).
 251



252
 253

254 **Figure 4.** Temperature dependence of (a) ammonia and (b-g) C1-C6 amines measured in Houston.
 255 Vertical bars indicate 1 standard deviation from the mean values of observation data. Binned
 256 temperatures are shown in colored squares, 1-minute averaged data is shown in gray squares.
 257 Horizontal bars indicate bin width. Black dashed lines indicate exponential fit for ammonia and
 258 linear fits for amines.

259 Anthropogenic pollutants such as CO and NO_x and CO can serve as tracers for industrial and
 260 traffic activities. Ammonia and amines in general showed a positive correlation with CO, with the
 261 exception of C3 amines (Figure 5). As ammonia, amines, and CO can be traced to traffic or
 262 industrial emissions, the positive relationship between these compounds implies that these base
 263 compounds were emitted from pollutant sources. Unlike with CO, there was a negative correlation
 264 with NO_x (Figure S3). This lack of a strong correlation between NO_x and ammonia was previously
 265 observed in Nanjing where a strong reduction in NO_x concentration during COVID-19 lockdown
 266 periods was not accompanied by an equivalent reduction in ammonia concentrations (Liu et al.,
 267 2024). This may indicate some unique emission sources for ammonia and amines that do not
 268 co-emit NO_x.
 269

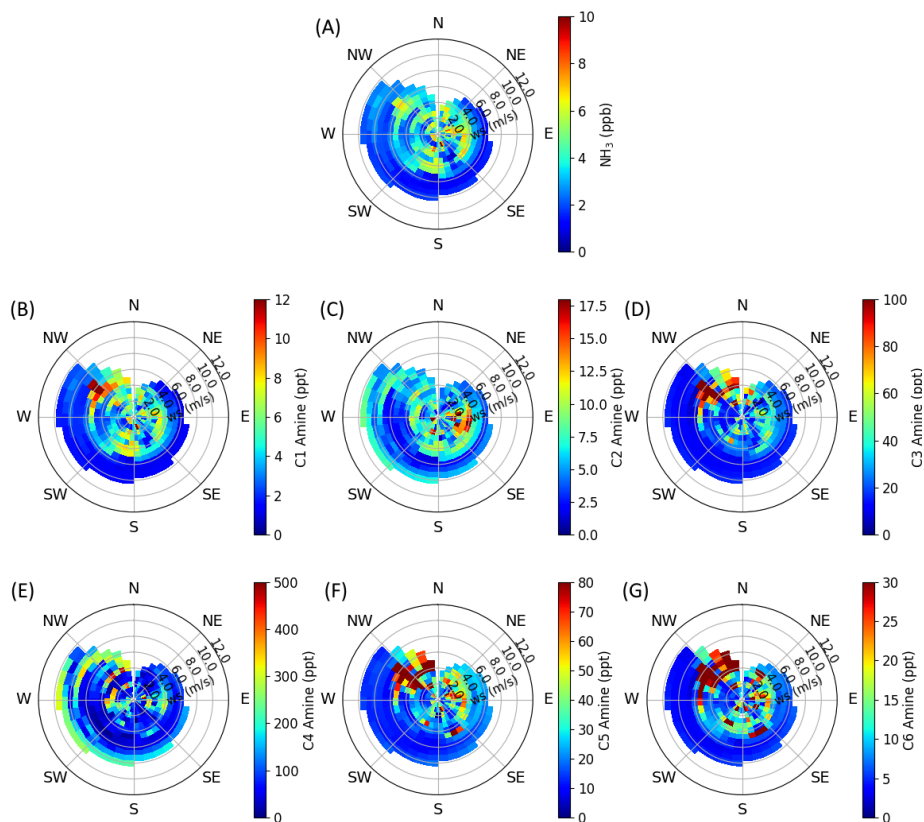


270
 271 **Figure 5.** Correlation between ammonia (a) and C1-C6 amines (b-g) with the collocated CO
 272 concentrations during the measurement campaign. Binned CO concentrations are shown in colored
 273 squares, 5-minute averaged data shown in gray squares. Vertical bars indicate 1 standard deviation
 274 from the mean values of observation data. Horizontal bars indicate bin widths. Black dashed lines
 275 indicate linear fits.

276 Wind speed and direction can help to identify local sources of ammonia and amines near the
 277 measurement site. Figures 6 and S4 show the correlation of ammonia and amines with wind speeds
 278 and direction throughout the observation period. Consistent between all base compounds is the
 279 high concentration coming from the southeast. This is the direction of the interstate highway,
 280 industrial areas, and train yards (Figures 1 and S1). Ammonia and most amines also have a
 281 pronounced source from the northwest – this is the direction of downtown Houston, where
 282 population density is highest. Except for C2 and C4 amines, the observed ammonia and amines in
 283 Houston were higher during periods of low wind speeds. The abundant C2 and C4 at high wind
 284 speeds may suggest that C2 and C4 amines were transported from more distant sources.

285 Figure S5 shows the average diurnal cycle of ammonia and amines on weekdays as opposed
 286 to weekends. Except for C2 and C4 amines, there was a clear decrease in concentrations during
 287 weekends during the afternoon peak. Weekends saw much less traffic and activity on the
 288 University of Houston campus. During this observation period, ambient temperatures were higher
 289 during the weekends, which would increase emissions. Therefore, the differences in weekdays vs.
 290 weekends indicate that amines and ammonia were indeed emitted from traffic and industrial
 291 activities. Lower average amine concentrations on weekends were also observed during mobile
 292 measurements in Yangtze River Delta cities (Chang et al., 2022).

293
 294

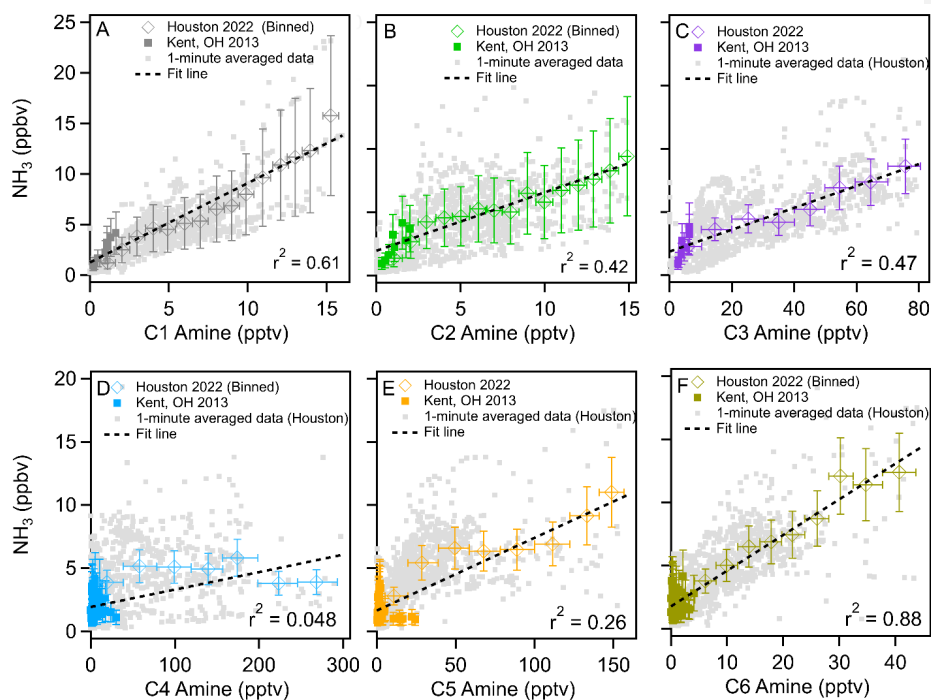


295
 296
 297 **Figure 6.** Wind rose plots of (a) ammonia and (b-g) C1-C6 amines observed in urban Houston.
 298 The color scale indicates concentration, and radial intensity shows wind speed.
 299

300 4. Atmospheric Implications

301
 302 Field observations show that sulfuric acid and amines are responsible for aerosol nucleation
 303 (Yao et al., 2016; Yan et al., 2021; Cai et al., 2021; Cai et al., 2023; Jen et al., 2016; Smith et al.,
 304 2010; Brean et al., 2020), however, currently, global models do not have amine emission
 305 inventories. Figure 7 shows the correlation of ammonia with C1-C6 amines measured during this
 306 campaign. This figure also includes that data obtained with the same instrument in Kent, Ohio,
 307 (You et al., 2014). It is clear from this figure that concentrations of ammonia, C1, C2, C3, C5, and
 308 C6 amines were positively correlated with one another throughout the study: r^2 values for the
 309 correlation between ammonia and amines were 0.61 for C1, 0.42 for C2, 0.47 for C3, 0.26 for C5

310 and 0.88 for C6. These relationships imply that these compounds are mostly co-emitted from
 311 similar sources and undergo similar atmospheric transport. C4 amines showed no correlation with
 312 ammonia and lower-mass amines – the r^2 value for C4 vs. NH_3 was 0.048. This indicates a unique
 313 source for C4 amines, consistent with both elevated C4 concentrations at high wind speeds and
 314 higher weekend C4 concentrations as discussed previously. Correlations of C1-C3 amines
 315 concentrations, taken from the linear fits of the plots shown in Figure 7, were approximately
 316 equivalent to 1.1×10^{-3} [NH_3], 1.4×10^{-3} [NH_3], and 8.4×10^{-3} [NH_3], respectively. C5 and C6
 317 amine concentrations were 1.9×10^{-2} [NH_3] and 3.5×10^{-3} [NH_3], respectively (Table S2). From
 318 these results, we propose that global modelers use 0.1 % of the ammonia concentration as a proxy
 319 of dimethylamine to simulate urban NPF processes. However, this recommendation comes with
 320 the caveat that measured C2 amines may include dimethylamine as well as ethylamine due to the
 321 inability of mass spectrometry to resolve isomers. Therefore, this correlation represents only the
 322 upper bound of dimethylamine concentrations.
 323



324
 325 **Figure 7.** Correlations of C1-C6 amines with ammonia throughout the observation period in
 326 Houston (diamonds) and Kent, OH (squares) as reported by (You et al., 2014). Binned
 327 concentrations are shown in colored squares, 1-minute averaged data from Houston are shown in

328 gray squares. Vertical bars indicate one standard deviation from the mean values of observation
329 data. Horizontal bars indicate bin widths. Black dashed lines indicate linear fits of the combined
330 data from Kent and Houston.

331 From these observations made in very polluted Houston and less polluted Kent, we propose
332 that at the polluted sites in the United States, dimethylamine concentrations can be estimated using
333 the proxy, 0.1% ammonia concentrations. The caveat of this proxy is that it is based on only two
334 locations in the United States and did not consider different emission sectors. There has been so
335 far only one attempt to use quantify the aerosol nucleation processes using sulfuric acid and
336 dimethylamine in the global model by Zhao et al. (Zhao et al., 2024) and they concluded that this
337 nucleation process is dominant globally in polluted boundary layer, from China, India, Europe to
338 United States. In this cited study the authors used the proxy of dimethylamine using ammonia
339 concentrations, for example, dimethylamine/ammonia ratio of 0.0070, 0.0018, and 0.0100, for
340 chemical industrial, other industrial, and residential sources; these proxies were derived by Mao
341 et al. (Mao et al., 2018) based on the measurement made in Nanjing (Zheng et al., 2015). Our
342 observations indicate that (Zhao et al., 2024) likely overestimated dimethylamine concentrations
343 for polluted sites in the United States overall, and thus overpredicted nucleation rates as well. Thus,
344 our results can provide more constrained proxy for polluted sites in the United States for future
345 modeling studies.

346 5. Conclusions

347 Our observations in urban Houston show that ammonia and amines generally followed a clear
348 diurnal cycle, peaking in the early afternoon when the ambient temperature was highest during the
349 day. We found a correlation between ammonia/amines and ambient temperature. The diurnal
350 cycles and temperature dependence of these compounds are consistent with (You et al., 2014)
351 which showed that the gas-to-particle conversion contributes to the temperature dependence. To
352 verify this process, the chemical composition of particle is needed, but particle measurements were
353 not available during the present study. Additionally, the observed temperature dependence could
354 be due to increased emissions of ammonia and amines from biogenic and anthropogenic sources.
355 On the other hand, photochemical aging that occurs typically during the higher solar flux can also
356 reduce the gas phase amines at the noontime; thus, photochemical aging was unlikely the main
357 driving factor to produce higher concentrations of amines around noon.

358 High concentrations of ammonia and amines were correlated with local air masses from
359 densely populated areas and areas of high traffic, industry, and other human activity. This suggests
360 that most ammonia and amines measured in Houston originated from pollutant sources, consistent
361 with the correlation observed with CO concentrations. There was also a clear increase in ammonia
362 and amines on days with more human activity as shown by the results of concentrations on
363 weekends vs weekdays. We observed a consistent relationship between ammonia and amines
364 during our measurement campaign as well as with observations in less densely populated Kent,
365 Ohio, suggesting that it is reasonable to parameterize amine emission inventories based on existing
366 ammonia inventories to simulate urban NPF processes. However, as the CIMS is incapable of

Formatted: Indent: First line: 0.25"

Deleted: of

Deleted: and

Deleted: with

Deleted: pronounced

Deleted: may be due to active partitioning between the gas and particle phases, which is sensitively dependent on temperature.

Deleted: T

Deleted: is

Deleted: It is likely a combination of these effects that causes elevated ammonia and amine concentrations when temperatures are high.

378 resolving amides or isomers, this parameterization is only capable of representing the upper
379 bounds of amines. Further work involving instrumentation capable of isomer resolution such as
380 tandem MS/MS or chromatographic separation is needed to determine typical isomer ratios of
381 amines for more accurate parameterizations.

382 Measuring ammonia and amines in the atmosphere is one of the most challenging areas in the
383 development of atmospheric analytical instruments (Lee, 2022; Lee et al., 2019). The CIMS used
384 in this campaign is currently one of the few instruments in the world that is capable of simultaneous
385 measurements of ammonia and amines at atmospherically relevant detection limits and timescales.
386 Very importantly, our CIMS, despite its relatively low mass resolution, has measured ammonia
387 and amines at various atmospheric conditions, ranging from the rural forests (You et al., 2014;
388 Kanawade et al., 2014), a relatively less polluted site (Yu and Lee, 2012 ; You et al., 2014; Erupe
389 et al., 2010), to the extremely polluted urban environment (this study), with consistent instrument
390 sensitivities over the decade; to our knowledge, this is the only instrument that demonstrated such
391 consistency in the performance. Studies have shown that the co-presence of ammonia and amines
392 can enhance sulfuric acid nucleation rates compared to ammonia alone (Yu et al., 2012; Glasoe et
393 al., 2015; Myllys et al., 2019). From this perspective, simultaneous measurements of ammonia and
394 amines will be required for the correct prediction of NPF processes in the atmosphere.
395 Measurements of ammonia and amines with comprehensive calibration as shown in the present
396 study are very even rarer, but such measurements are needed for mitigating urban air quality
397 problems and the health effects of ultrafine particles.

399 **Author Contributions**

400 SHL designed the research; LT and SHL performed measurements; JF provided the measurement
401 platform as well as the trace gas and meteorology data; LT and SHL wrote the manuscript.

402 **Competing interests**

403 The authors declare that they have no conflict of interest.

404 **Acknowledgements**

405 We acknowledge funding support from National Science Foundation (grant numbers 2209722,
406 2117389, and 2107916) and Texas Commission on Environmental Quality (grant number 582-22-
407 31535-018).

408

409 **Table 1.** Ammonia and amine measurements with CIMS at various locations reported in the
 410 literature. DL, detection limit of each instrument.

Location	NH ₃ (ppbv)	C1 Amine (pptv)	C2 Amine (pptv)	C3 Amine (pptv)	C4 Amine (pptv)	C5 Amine (pptv)	C6 Amine (pptv)
Rural Alabama Forest (You et al., 2014)*	Up to 1-2	< DL	< DL	1 - 10	< DL	< DL	< DL
Kent, Ohio (You et al., 2014)*	Up to 6	1 – 4	< DL	5 - 10	10 - 50	10 - 100	< DL
Kent, Ohio (Yu and Lee, 2012)*	0.5 ± 0.26	-	8 ± 3	16 ± 7	-	-	-
Atlanta, Georgia (Hanson et al., 2011)†	-	< 1	3	4 – 15	25	-	-
Lewes, Delaware (Freshour et al., 2014)†	0.8	5	28	6	150	1	2
Lamont, Oklahoma (Freshour et al., 2014)†	0.9	4	14	35	150	98	20
Minneapolis, Minnesota (Freshour et al., 2014)†	1.8	4	42	19	14	20	5
Shanghai (Yao et al., 2016)‡	-	3.9 ± 1.2	6.6 ± 1.2	0.4 ± 0.1	3.6 ± 1.0	0.7 ± 0.3	1.8 ± 0.8
Nanjing (Zheng et al., 2015)‡	1.7 ± 2.3	7.2 ± 7.4 (C1 + C2 + C3)			-	-	-
Wangdu	-	-	14.6 ± 14.9	-	-	-	-

(Wang et al., 2020b)§							
Beijing (Zhu et al., 2022)‡	2.8 ± 2.0	5.2 ± 4.3 (C1 + C2 + C3)	-	-	-		
Houston, TX (This study)*	4 ± 1	4 ± 2	6 ± 2	31 ± 9	79 ± 30	33 ± 12	12 ± 4

411
412 * CIMS with ethanol reagent
413 † Proton-transfer chemical ionization mass spectrometer (PTR-CIMS)
414 ‡ High-resolution time of flight chemical ionization mass spectrometer (HR-TOF CIMS) with
415 ethanol reagent
416 § Vocus proton transfer time-of-flight mass spectrometer (PTR-TOF MS)
417
418

419 **References**

- 420
- 421 Almeida, J., Schobesberger, S., Kürten, A., Ortega, I. K., Kupiainen-Määttä, O., Praplan, A. P.,
422 Adamov, A., Amorim, A., Bianchi, F., Breitenlechner, M., David, A., Dommen, J.,
423 Donahue, N. M., Downard, A., Dunne, E., Duplissy, J., Ehrhart, S., Flagan, R. C.,
424 Franchin, A., Guida, R., Hakala, J., Hansel, A., Heinritzi, M., Henschel, H., Jokinen, T.,
425 Junninen, H., Kajos, M., Kangasluoma, J., Keskinen, H., Kupc, A., Kurtén, T., Kvashin,
426 A. N., Laaksonen, A., Lehtipalo, K., Leiminger, M., Leppä, J., Loukonen, V.,
427 Makhmutov, V., Mathot, S., McGrath, M. J., Nieminen, T., Olenius, T., Onnela, A.,
428 Petäjä, T., Riccobono, F., Riipinen, I., Rissanen, M., Rondo, L., Ruuskanen, T., Santos,
429 F. D., Sarnela, N., Schallhart, S., Schnitzhofer, R., Seinfeld, J. H., Simon, M., Sipilä, M.,
430 Stozhkov, Y., Stratmann, F., Tomé, A., Tröstl, J., Tsagkogeorgas, G., Vaattovaara, P.,
431 Viisanen, Y., Virtanen, A., Vrtala, A., Wagner, P. E., Weingartner, E., Wex, H.,
432 Williamson, C., Wimmer, D., Ye, P., Yli-Juuti, T., Carslaw, K. S., Kulmala, M., Curtius,
433 J., Baltensperger, U., Worsnop, D. R., Vehkamäki, H., and Kirkby, J.: Molecular
434 understanding of sulphuric acid-amine particle nucleation in the atmosphere, *Nature*,
435 502, 359-363, 10.1038/nature12663, 2013.
- 436 Beck, L. J., Sarnela, N., Junninen, H., Hoppe, C. J. M., Garmash, O., Bianchi, F., Riva, M., Rose,
437 C., Peräkylä, O., Wimmer, D., Kausiala, O., Jokinen, T., Ahonen, L., Mikkilä, J., Hakala,
438 J., He, X.-C., Kontkanen, J., Wolf, K. K. E., Cappelletti, D., Mazzola, M., Traversi, R.,
439 Petroselli, C., Viola, A. P., Vitale, V., Lange, R., Massling, A., Nøjgaard, J. K., Krejci,
440 R., Karlsson, L., Zieger, P., Jang, S., Lee, K., Vakkari, V., Lampilahti, J., Thakur, R. C.,
441 Leino, K., Kangasluoma, J., Duplissy, E.-M., Siivola, E., Marbouti, M., Tham, Y. J.,
442 Saiz-Lopez, A., Petäjä, T., Ehn, M., Worsnop, D. R., Skov, H., Kulmala, M., Kerminen,
443 V.-M., and Sipilä, M.: Differing Mechanisms of New Particle Formation at Two Arctic
444 Sites, *Geophysical Research Letters*, 48, e2020GL091334,
445 <https://doi.org/10.1029/2020GL091334>, 2021.
- 446 Benson, D. R., Markovich, A., Al-Refai, M., and Lee, S. H.: A Chemical Ionization Mass
447 Spectrometer for ambient measurements of Ammonia, *Atmos. Meas. Tech.*, 3, 1075-
448 1087, 10.5194/amt-3-1075-2010, 2010.
- 449 Bianchi, F., Tröstl, J., Junninen, H., Frege, C., Henne, S., Hoyle, C. R., Molteni, U., Herrmann,
450 E., Adamov, A., Bukowiecki, N., Chen, X., Duplissy, J., Gysel, M., Hutterli, M.,
451 Kangasluoma, J., Kontkanen, J., Kürten, A., Manninen, H. E., Münch, S., Peräkylä, O.,
452 Petäjä, T., Rondo, L., Williamson, C., Weingartner, E., Curtius, J., Worsnop, D. R.,
453 Kulmala, M., Dommen, J., and Baltensperger, U.: New particle formation in the free
454 troposphere: A question of chemistry and timing, *Science*, 352, 1109-1112,
455 10.1126/science.aad5456, 2016.
- 456 Brean, J., Dall'Osto, M., Simó, R., Shi, Z., Beddows, D. C. S., and Harrison, R. M.: Open ocean
457 and coastal new particle formation from sulfuric acid and amines around the Antarctic
458 Peninsula, *Nature Geoscience*, 14, 383-388, 10.1038/s41561-021-00751-y, 2021.
- 459 Brean, J., Beddows, D. C. S., Shi, Z., Temime-Roussel, B., Marchand, N., Querol, X., Alastuey,
460 A., Minguillón, M. C., and Harrison, R. M.: Molecular insights into new particle
461 formation in Barcelona, Spain, *Atmos. Chem. Phys.*, 20, 10029-10045, 10.5194/acp-20-
462 10029-2020, 2020.
- 463 Cai, R., Yin, R., Li, X., Xie, H.-B., Yang, D., Kerminen, V.-M., Smith, J. N., Ma, Y., Hao, J.,
464 Chen, J., Kulmala, M., Zheng, J., Jiang, J., and Elm, J.: Significant contributions of

Formatted: Indent: Left: 0", Hanging: 0.5"

465 trimethylamine to sulfuric acid nucleation in polluted environments, *npj Climate and*
466 *Atmospheric Science*, 6, 75, 10.1038/s41612-023-00405-3, 2023.

467 Cai, R., Yan, C., Yang, D., Yin, R., Lu, Y., Deng, C., Fu, Y., Ruan, J., Li, X., Kontkanen, J.,
468 Zhang, Q., Kangasluoma, J., Ma, Y., Hao, J., Worsnop, D. R., Bianchi, F., Paasonen, P.,
469 Kerminen, V. M., Liu, Y., Wang, L., Zheng, J., Kulmala, M., and Jiang, J.: Sulfuric acid-
470 amine nucleation in urban Beijing, *Atmos. Chem. Phys.*, 21, 2457-2468, 10.5194/acp-21-
471 2457-2021, 2021.

472 Chang, Y., Wang, H., Gao, Y., Jing, S. a., Lu, Y., Lou, S., Kuang, Y., Cheng, K., Ling, Q., Zhu,
473 L., Tan, W., and Huang, R.-J.: Nonagricultural Emissions Dominate Urban Atmospheric
474 Amines as Revealed by Mobile Measurements, *Geophysical Research Letters*, 49,
475 e2021GL097640, <https://doi.org/10.1029/2021GL097640>, 2022.

476 Ellis, R. A., Murphy, J. G., Pattey, E., van Haarlem, R., O'Brien, J. M., and Herndon, S. C.:
477 Characterizing a Quantum Cascade Tunable Infrared Laser Differential Absorption
478 Spectrometer (QC-TILDAS) for measurements of atmospheric ammonia, *Atmos. Meas.*
479 *Tech.*, 3, 397-406, 10.5194/amt-3-397-2010, 2010.

480 Erupe, M. E., Viggiano, A. A., and Lee, S. H.: The effect of trimethylamine on atmospheric
481 nucleation involving H₂SO₄, *Atmos. Chem. Phys.*, 11, 4767-4775, 2011.

482 Erupe, M. E., Benson, D. R., Li, J., Young, L.-H., Verheggen, B., Al-Refai, M., Tahboub, O.,
483 Cunningham, V., Frimpong, F., Viggiano, A. A., and Lee, S.-H.: Correlation of aerosol
484 nucleation rate with sulfuric acid and ammonia in Kent, Ohio: An atmospheric
485 observation, *Journal of Geophysical Research: Atmospheres*, 115,
486 <https://doi.org/10.1029/2010JD013942>, 2010.

487 Freshour, N. A., Carlson, K. K., Melka, Y. A., Hinz, S., Panta, B., and Hanson, D. R.: Amine
488 permeation sources characterized with acid neutralization and sensitivities of an amine
489 mass spectrometer, *Atmos. Meas. Tech.*, 7, 3611-3621, 10.5194/amt-7-3611-2014, 2014.

490 Ge, X., Wexler, A. S., and Clegg, S. L.: Atmospheric amines – Part I. A review, *Atmospheric*
491 *Environment*, 45, 524-546, <https://doi.org/10.1016/j.atmosenv.2010.10.012>, 2011a.

492 Ge, X., Wexler, A. S., and Clegg, S. L.: Atmospheric amines – Part II. Thermodynamic
493 properties and gas/particle partitioning, *Atmospheric Environment*, 45, 561-577,
494 <https://doi.org/10.1016/j.atmosenv.2010.10.013>, 2011b.

495 Glasoe, W. A., Volz, K., Panta, B., Freshour, N., Bachman, R., Hanson, D. R., McMurry, P. H.,
496 and Jen, C.: Sulfuric acid nucleation: an experimental study of the effect of seven bases,
497 *J. Geophys. Res.*, 120, 1933-1950, Doi: 10.1002/2014JD022730, 2015.

498 Griffith, D. W. T. and Galle, B.: Flux measurements of NH₃, N₂O and CO₂ using dual beam
499 FTIR spectroscopy and the flux-gradient technique, *Atmospheric Environment*, 34,
500 1087-1098, [https://doi.org/10.1016/S1352-2310\(99\)00368-4](https://doi.org/10.1016/S1352-2310(99)00368-4), 2000.

501 Gu, B., Zhang, L., Van Dingenen, R., Vieno, M., Van Grinsven, H. J. M., Zhang, X., Zhang, S.,
502 Chen, Y., Wang, S., Ren, C., Rao, S., Holland, M., Winiwarter, W., Chen, D., Xu, J., and
503 Sutton, M. A.: Abating ammonia is more cost-effective than nitrogen oxides for
504 mitigating PM_{2.5} air pollution, *Science*, 374, 758-762, 10.1126/science.abf8623, 2021.

505 Hanson, D. R., McMurry, P. H., Jiang, J., Tanner, D., and Huey, L. G.: Ambient Pressure Proton
506 Transfer Mass Spectrometry: Detection of Amines and Ammonia, *Environmental Science*
507 *& Technology*, 45, 8881-8888, 10.1021/es201819a, 2011.

508 Jen, C. N., Bachman, R., Zhao, J., McMurry, P. H., and Hanson, D. R.: Diamine-sulfuric acid
509 reactions are a potent source of new particle formation, *Geophysical Research Letters*,
510 43, 867-873, <https://doi.org/10.1002/2015GL066958>, 2016.

- 511 Jokinen, T., Sipilä, M., Kontkanen, J., Vakkari, V., Tisler, P., Duplissy, E. M., Junninen, H.,
 512 Kangasluoma, J., Manninen, H. E., Petäjä, T., Kulmala, M., Worsnop, D. R., Kirkby, J.,
 513 Virkkula, A., and Kerminen, V. M.: Ion-induced sulfuric acid–ammonia nucleation drives
 514 particle formation in coastal Antarctica, *Science Advances*, 4, eaat9744,
 515 10.1126/sciadv.aat9744,
- 516 Kanawade, V. P., Tripathi, S. N., Siingh, D., Gautam, A. S., Srivastava, A. K., Kamra, A. K.,
 517 Soni, V. K., and Sethi, V.: Observations of new particle formation at two distinct Indian
 518 subcontinental urban locations, *Atmos. Environ.*, 96, 370-379, Doi:
 519 10.1016/j.atmosenv.2014.08.001, 2014.
- 520 Köllner, F., Schneider, J., Willis, M. D., Klimach, T., Helleis, F., Bozem, H., Kunkel, D., Hoor,
 521 P., Burkart, J., Leaitch, W. R., Aliabadi, A. A., Abbatt, J. P. D., Herber, A. B., and
 522 Borrmann, S.: Particulate trimethylamine in the summertime Canadian high Arctic lower
 523 troposphere, *Atmos. Chem. Phys.*, 17, 13747-13766, 10.5194/acp-17-13747-2017, 2017.
- 524 Kürten, A., Bergen, A., Heinritzi, M., Leiminger, M., Lorenz, V., Piel, F., Simon, M., Sitals, R.,
 525 Wagner, A. C., and Curtius, J.: Observation of new particle formation and measurement
 526 of sulfuric acid, ammonia, amines and highly oxidized organic molecules at a rural site in
 527 central Germany, *Atmos. Chem. Phys.*, 16, 12793-12813, 10.5194/acp-16-12793-2016,
 528 2016.
- 529 Lee, S.-H.: Perspective on the Recent Measurements of Reduced Nitrogen Compounds in the
 530 Atmosphere, *Frontiers in Environmental Science*, 10, 10.3389/fenvs.2022.868534, 2022.
- 531 Lee, S.-H., Gordon, H., Yu, H., Lehtipalo, K., Haley, R., Li, Y., and Zhang, R.: New Particle
 532 Formation in the Atmosphere: From Molecular Clusters to Global Climate, *Journal of
 533 Geophysical Research: Atmospheres*, 124, 7098-7146, 10.1029/2018JD029356, 2019.
- 534 Leen, J. B., Yu, X.-Y., Gupta, M., Baer, D. S., Hubbe, J. M., Kluzek, C. D., Tomlinson, J. M.,
 535 and Hubbell, M. R., II: Fast In Situ Airborne Measurement of Ammonia Using a Mid-
 536 Infrared Off-Axis ICOS Spectrometer, *Environmental Science & Technology*, 47, 10446-
 537 10453, 10.1021/es401134u, 2013.
- 538 Lehtipalo, K., Yan, C., Dada, L., Bianchi, F., Xiao, M., Wagner, R., Stolzenburg, D., Ahonen, L.
 539 R., Amorim, A., Baccarini, A., Bauer, P. S., Baumgartner, B., Bergen, A., Bernhammer,
 540 A.-K., Breitenlechner, M., Brilke, S., Buchholz, A., Mazon, S. B., Chen, D., Chen, X.,
 541 Dias, A., Dommen, J., Draper, D. C., Duplissy, J., Ehn, M., Finkenzeller, H., Fischer, L.,
 542 Frege, C., Fuchs, C., Garmash, O., Gordon, H., Hakala, J., He, X., Heikkinen, L.,
 543 Heinritzi, M., Helm, J. C., Hofbauer, V., Hoyle, C. R., Jokinen, T., Kangasluoma, J.,
 544 Kerminen, V.-M., Kim, C., Kirkby, J., Kontkanen, J., Kürten, A., Lawler, M. J., Mai, H.,
 545 Mathot, S., Mauldin, R. L., Molteni, U., Nichman, L., Nie, W., Nieminen, T., Ojdanic,
 546 A., Onnela, A., Passananti, M., Petäjä, T., Piel, F., Pospisilova, V., Quéléver, L. L. J.,
 547 Rissanen, M. P., Rose, C., Sarnela, N., Schallhart, S., Schuchmann, S., Sengupta, K.,
 548 Simon, M., Sipilä, M., Tauber, C., Tomé, A., Tröstl, J., Väisänen, O., Vogel, A. L.,
 549 Volkamer, R., Wagner, A. C., Wang, M., Weitz, L., Wimmer, D., Ye, P., Ylisirmä, A.,
 550 Zha, Q., Carslaw, K. S., Curtius, J., Donahue, N. M., Flagan, R. C., Hansel, A., Riipinen,
 551 I., Virtanen, A., Winkler, P. M., Baltensperger, U., Kulmala, M., and Worsnop, D. R.:
 552 Multicomponent new particle formation from sulfuric acid, ammonia, and biogenic
 553 vapors, *Science Advances*, 4, eaau5363, 10.1126/sciadv.aau5363, 2018.
- 554 Liu, R., Liu, T., Huang, X., Ren, C., Wang, L., Niu, G., Yu, C., Zhang, Y., Wang, J., Qi, X., Nie,
 555 W., Chi, X., and Ding, A.: Characteristics and sources of atmospheric ammonia at the

556 SORPES station in the western Yangtze river delta of China, *Atmospheric Environment*,
557 318, 120234, <https://doi.org/10.1016/j.atmosenv.2023.120234>, 2024.

558 Malloy, Q. G. J., Li, Q., Warren, B., Cocker Iii, D. R., Erupe, M. E., and Silva, P. J.: Secondary
559 organic aerosol formation from primary aliphatic amines with NO₃ radical,
560 *Atmos. Chem. Phys.*, 9, 2051-2060, 10.5194/acp-9-2051-2009, 2009.

561 Mao, J., Yu, F., Zhang, Y., An, J., Wang, L., Zheng, J., Yao, L., Luo, G., Ma, W., Yu, Q.,
562 Huang, C., Li, L., and Chen, L.: High-resolution modeling of gaseous methylamines over
563 a polluted region in China: source-dependent emissions and implications of spatial
564 variations, *Atmos. Chem. Phys.*, 18, 7933-7950, 10.5194/acp-18-7933-2018, 2018.

565 Martin, N. A., Ferracci, V., Cassidy, N., and Hoffnagle, J. A.: The application of a cavity ring-
566 down spectrometer to measurements of ambient ammonia using traceable primary
567 standard gas mixtures, *Applied Physics B*, 122, 219, 10.1007/s00340-016-6486-9, 2016.

568 McManus, J. B., Mark, S. Z., David, D. N., Jr., Joanne, H. S., Scott, C. H., Ezra, C. W., and
569 Rick, W.: Application of quantum cascade lasers to high-precision atmospheric trace gas
570 measurements, *Optical Engineering*, 49, 111124, 10.1117/1.3498782, 2010.

571 Miller, D. J., Sun, K., Tao, L., Khan, M. A., and Zondlo, M. A.: Open-path, quantum cascade-
572 laser-based sensor for high-resolution atmospheric ammonia measurements, *Atmos.*
573 *Meas. Tech.*, 7, 81-93, 10.5194/amt-7-81-2014, 2014.

574 Myllys, N., Chee, S., Olenius, T., Lawler, M., and Smith, J.: Molecular-Level Understanding of
575 Synergistic Effects in Sulfuric Acid–Amine–Ammonia Mixed Clusters, *The Journal of*
576 *Physical Chemistry A*, 123, 2420-2425, 10.1021/acs.jpca.9b00909, 2019.

577 Nielsen, C. J.: Atmospheric Degradation of Amines (ADA). Summary report: Photo-oxidation of
578 methylamine, dimethylamine and trimethylamine. CLIMIT project no. 201604., Norge:
579 Norsk Institutt for Luftforskning, 2016.

580 Nielsen, C. J., Herrmann, H., and Weller, C.: Atmospheric chemistry and environmental impact
581 of the use of amines in carbon capture and storage (CCS), *Chemical Society Reviews*, 41,
582 6684-6704, 10.1039/C2CS35059A, 2012.

583 Nowak, J. B., Neuman, J. A., Bahreini, R., Brock, C. A., Middlebrook, A. M., Wollny, A. G.,
584 Holloway, J. S., Peischl, J., Ryerson, T. B., and Fehsenfeld, F. C.: Airborne observations
585 of ammonia and ammonium nitrate formation over Houston, Texas, *Journal of*
586 *Geophysical Research: Atmospheres*, 115, <https://doi.org/10.1029/2010JD014195>, 2010.

587 Nowak, J. B., Huey, L. G., Russell, A. G., Tian, D., Neuman, J. A., Orsini, D., Sjostedt, S. J.,
588 Sullivan, A. P., Tanner, D. J., Weber, R. J., Nenes, A., Edgerton, E., and Fehsenfeld, F.
589 C.: Analysis of urban gas phase ammonia measurements from the 2002 Atlanta Aerosol
590 Nucleation and Real-Time Characterization Experiment (ANARChE), *Journal of*
591 *Geophysical Research: Atmospheres*, 111, <https://doi.org/10.1029/2006JD007113>, 2006.

592 Petrus, M., Popa, C., and Bratu, A. M.: Ammonia Concentration in Ambient Air in a Peri-Urban
593 Area Using a Laser Photoacoustic Spectroscopy Detector, *Materials (Basel)*, 15,
594 10.3390/ma15093182, 2022.

595 Pollack, I. B., Lindaas, J., Roscioli, J. R., Agnese, M., Permar, W., Hu, L., and Fischer, E. V.:
596 Evaluation of ambient ammonia measurements from a research aircraft using a closed-
597 path QC-TILDAS operated with active continuous passivation, *Atmos. Meas. Tech.*, 12,
598 3717-3742, 10.5194/amt-12-3717-2019, 2019.

599 Pushkarsky, M. B., Webber, M. E., Baghdassarian, O., Narasimhan, L. R., and Patel, C. K. N.:
600 Laser-based photoacoustic ammonia sensors for industrial applications, *Applied Physics*
601 *B*, 75, 391-396, 10.1007/s00340-002-0967-8, 2002.

- 602 Qiu, C. and Zhang, R.: Multiphase chemistry of atmospheric amines, *Physical Chemistry*
603 *Chemical Physics*, 15, 5738-5752, 10.1039/C3CP43446J, 2013.
- 604 Schwab, J. J., Li, Y., Bae, M. S., Demerjian, K. L., Hou, J., Zhou, X., Jensen, B., and Pryor, S.
605 C.: A laboratory intercomparison of real-time gaseous ammonia measurement methods,
606 *Environ Sci Technol*, 41, 8412-8419, 10.1021/es070354r, 2007.
- 607 Silva, P. J., Erupe, M. E., Price, D., Elias, J., G. J. Malloy, Q., Li, Q., Warren, B., and Cocker, D.
608 R., III: Trimethylamine as Precursor to Secondary Organic Aerosol Formation via Nitrate
609 Radical Reaction in the Atmosphere, *Environmental Science & Technology*, 42, 4689-
610 4696, 10.1021/es703016v, 2008.
- 611 Smith, J. N., Barsanti, K. C., Friedli, H. R., Ehn, M., Kulmala, M., Collins, D. R., Scheckman, J.
612 H., Williams, B. J., and McMurry, P. H.: Observations of ammonium salts in atmospheric
613 nanoparticles and possible climatic implications, *Proc. Natl. Acad. Sci.*, 107, 6634-6639,
614 2010.
- 615 Wang, G., Zhang, R., Gomez, M. E., Yang, L., Levy Zamora, M., Hu, M., Lin, Y., Peng, J., Guo,
616 S., Meng, J., Li, J., Cheng, C., Hu, T., Ren, Y., Wang, Y., Gao, J., Cao, J., An, Z., Zhou,
617 W., Li, G., Wang, J., Tian, P., Marrero-Ortiz, W., Secret, J., Du, Z., Zheng, J., Shang,
618 D., Zeng, L., Shao, M., Wang, W., Huang, Y., Wang, Y., Zhu, Y., Li, Y., Hu, J., Pan, B.,
619 Cai, L., Cheng, Y., Ji, Y., Zhang, F., Rosenfeld, D., Liss, P. S., Duce, R. A., Kolb, C. E.,
620 and Molina, M. J.: Persistent sulfate formation from London Fog to Chinese haze,
621 *Proceedings of the National Academy of Sciences*, 113, 13630-13635,
622 10.1073/pnas.1616540113, 2016.
- 623 Wang, M., Kong, W., Marten, R., He, X.-C., Chen, D., Pfeifer, J., Heitto, A., Kontkanen, J.,
624 Dada, L., Kürten, A., Yli-Juuti, T., Manninen, H. E., Amanatidis, S., Amorim, A.,
625 Baalbaki, R., Baccarini, A., Bell, D. M., Bertozzi, B., Bräkling, S., Brilke, S., Murillo, L.
626 C., Chiu, R., Chu, B., De Menezes, L.-P., Duplissy, J., Finkenzeller, H., Carracedo, L. G.,
627 Granzin, M., Guida, R., Hansel, A., Hofbauer, V., Krechmer, J., Lehtipalo, K.,
628 Lamkaddam, H., Lampimäki, M., Lee, C. P., Makhmutov, V., Marie, G., Mathot, S.,
629 Mauldin, R. L., Mentler, B., Müller, T., Onnela, A., Partoll, E., Petäjä, T., Philippov, M.,
630 Pospisilova, V., Ranjithkumar, A., Rissanen, M., Rörup, B., Scholz, W., Shen, J., Simon,
631 M., Sipilä, M., Steiner, G., Stolzenburg, D., Tham, Y. J., Tomé, A., Wagner, A. C.,
632 Wang, D. S., Wang, Y., Weber, S. K., Winkler, P. M., Wlasits, P. J., Wu, Y., Xiao, M.,
633 Ye, Q., Zauner-Wieczorek, M., Zhou, X., Volkamer, R., Riipinen, I., Dommen, J.,
634 Curtius, J., Baltensperger, U., Kulmala, M., Worsnop, D. R., Kirkby, J., Seinfeld, J. H.,
635 El-Haddad, I., Flagan, R. C., and Donahue, N. M.: Rapid growth of new atmospheric
636 particles by nitric acid and ammonia condensation, *Nature*, 581, 184-189,
637 10.1038/s41586-020-2270-4, 2020a.
- 638 Wang, Y., Yang, G., Lu, Y., Liu, Y., Chen, J., and Wang, L.: Detection of gaseous
639 dimethylamine using vocus proton-transfer-reaction time-of-flight mass spectrometry,
640 *Atmospheric Environment*, 243, 117875,
641 <https://doi.org/10.1016/j.atmosenv.2020.117875>, 2020b.
- 642 Xiao, M., Hoyle, C. R., Dada, L., Stolzenburg, D., Kürten, A., Wang, M., Lamkaddam, H.,
643 Garmash, O., Mentler, B., Molteni, U., Baccarini, A., Simon, M., He, X. C., Lehtipalo,
644 K., Ahonen, L. R., Baalbaki, R., Bauer, P. S., Beck, L., Bell, D., Bianchi, F., Brilke, S.,
645 Chen, D., Chiu, R., Dias, A., Duplissy, J., Finkenzeller, H., Gordon, H., Hofbauer, V.,
646 Kim, C., Koenig, T. K., Lampilahti, J., Lee, C. P., Li, Z., Mai, H., Makhmutov, V.,
647 Manninen, H. E., Marten, R., Mathot, S., Mauldin, R. L., Nie, W., Onnela, A., Partoll, E.,

648 Petäjä, T., Pfeifer, J., Pospisilova, V., Quéléver, L. L. J., Rissanen, M., Schobesberger, S.,
649 Schuchmann, S., Stozhkov, Y., Tauber, C., Tham, Y. J., Tomé, A., Vazquez-Pufleau, M.,
650 Wagner, A. C., Wagner, R., Wang, Y., Weitz, L., Wimmer, D., Wu, Y., Yan, C., Ye, P.,
651 Ye, Q., Zha, Q., Zhou, X., Amorim, A., Carslaw, K., Curtius, J., Hansel, A., Volkamer,
652 R., Winkler, P. M., Flagan, R. C., Kulmala, M., Worsnop, D. R., Kirkby, J., Donahue, N.
653 M., Baltensperger, U., El Haddad, I., and Dommen, J.: The driving factors of new particle
654 formation and growth in the polluted boundary layer, *Atmos. Chem. Phys.*, 21, 14275-
655 14291, 10.5194/acp-21-14275-2021, 2021.

656 Xiao, S., Wang, M. Y., Yao, L., Kulmala, M., Zhou, B., Yang, X., Chen, J. M., Wang, D. F., Fu,
657 Q. Y., Worsnop, D. R., and Wang, L.: Strong atmospheric new particle formation in
658 winter in urban Shanghai, China, *Atmos. Chem. Phys.*, 15, 1769-1781, 10.5194/acp-15-
659 1769-2015, 2015.

660 Yan, C., Yin, R., Lu, Y., Dada, L., Yang, D., Fu, Y., Kontkanen, J., Deng, C., Garmash, O.,
661 Ruan, J., Baalbaki, R., Schervish, M., Cai, R., Bloss, M., Chan, T., Chen, T., Chen, Q.,
662 Chen, X., Chen, Y., Chu, B., Dällenbach, K., Foreback, B., He, X., Heikkinen, L.,
663 Jokinen, T., Junninen, H., Kangasluoma, J., Kokkonen, T., Kurppa, M., Lehtipalo, K., Li,
664 H., Li, H., Li, X., Liu, Y., Ma, Q., Paasonen, P., Rantala, P., Pileci, R. E., Rusanen, A.,
665 Sarnela, N., Simonen, P., Wang, S., Wang, W., Wang, Y., Xue, M., Yang, G., Yao, L.,
666 Zhou, Y., Kujansuu, J., Petäjä, T., Nie, W., Ma, Y., Ge, M., He, H., Donahue, N. M.,
667 Worsnop, D. R., Veli-Matti, K., Wang, L., Liu, Y., Zheng, J., Kulmala, M., Jiang, J., and
668 Bianchi, F.: The Synergistic Role of Sulfuric Acid, Bases, and Oxidized Organics
669 Governing New-Particle Formation in Beijing, *Geophysical Research Letters*, 48,
670 e2020GL091944, <https://doi.org/10.1029/2020GL091944>, 2021.

671 Yao, L., Wang, M. Y., Wang, X. K., Liu, Y. J., Chen, H. F., Zheng, J., Nie, W., Ding, A. J.,
672 Geng, F. H., Wang, D. F., Chen, J. M., Worsnop, D. R., and Wang, L.: Detection of
673 atmospheric gaseous amines and amides by a high-resolution time-of-flight chemical
674 ionization mass spectrometer with protonated ethanol reagent ions, *Atmos. Chem. Phys.*,
675 16, 14527-14543, 10.5194/acp-16-14527-2016, 2016.

676 You, Y., Kanawade, V. P., de Gouw, J. A., Guenther, A. B., Madronich, S., Sierra-Hernández,
677 M. R., Lawler, M., Smith, J. N., Takahama, S., Ruggeri, G., Koss, A., Olson, K.,
678 Baumann, K., Weber, R. J., Nenes, A., Guo, H., Edgerton, E. S., Porcelli, L., Brune, W.
679 H., Goldstein, A. H., and Lee, S. H.: Atmospheric amines and ammonia measured with a
680 Chemical Ionization Mass Spectrometer (CIMS), *Atmos. Chem. Phys.*, 14, 12181-
681 12194, Doi: 10.5194/acpd-14-16411-2014, 2014.

682 Yu, H. and Lee, S. H.: A chemical ionization mass spectrometer for the detection of atmospheric
683 amines, *Environ. Chem.*, 9, 190-201, 2012

684 Yu, H., McGraw, R., and Lee, S. H.: Effects of amines on formation of sub-3 nm particles and
685 their subsequent growth, *Geophys. Res. Lett.*, 39, Doi: 10.1029/2011gl050099,
686 10.1029/2011gl050099, 2012.

687 Zhao, B., Donahue, N. M., Zhang, K., Mao, L., Shrivastava, M., Ma, P.-L., Shen, J., Wang, S.,
688 Sun, J., Gordon, H., Tang, S., Fast, J., Wang, M., Gao, Y., Yan, C., Singh, B., Li, Z.,
689 Huang, L., Lou, S., Lin, G., Wang, H., Jiang, J., Ding, A., Nie, W., Qi, X., Chi, X., and
690 Wang, L.: Global variability in atmospheric new particle formation mechanisms, *Nature*,
691 631, 98-105, 10.1038/s41586-024-07547-1, 2024.

692 Zheng, J., Ma, Y., Chen, M., Zhang, Q., Wang, L., Khalizov, A. F., Yao, L., Wang, Z., Wang,
693 X., and Chen, L.: Measurement of atmospheric amines and ammonia using the high

694 resolution time-of-flight chemical ionization mass spectrometry, Atmospheric
695 Environment, 102, 249-259, <https://doi.org/10.1016/j.atmosenv.2014.12.002>, 2015.
696 Zhu, S., Yan, C., Zheng, J., Chen, C., Ning, H., Yang, D., Wang, M., Ma, Y., Zhan, J., Hua, C.,
697 Yin, R., Li, Y., Liu, Y., Jiang, J., Yao, L., Wang, L., Kulmala, M., and Worsnop, D. R.:
698 Observation and Source Apportionment of Atmospheric Alkaline Gases in Urban
699 Beijing, Environmental Science & Technology, 56, 17545-17555,
700 10.1021/acs.est.2c03584, 2022.
701